Accepted Article

Title: Stimuli-responsive supramolecular polymers from amphiphilic phosphodiester-linked azobenzene trimers

Authors: Robert Häner, Oleh Vybornyi, and Shi-Xia Liu

This manuscript has been accepted after peer review and appears as an Accepted Article online prior to editing, proofing, and formal publication of the final Version of Record (VoR). This work is currently citable by using the Digital Object Identifier (DOI) given below. The VoR will be published online in Early View as soon as possible and may be different to this Accepted Article as a result of editing. Readers should obtain the VoR from the journal website shown below when it is published to ensure accuracy of information. The authors are responsible for the content of this Accepted Article.

To be cited as: *Angew. Chem. Int. Ed.* 10.1002/anie.202108745

Link to VoR: https://doi.org/10.1002/anie.202108745

WILEY-VCH

WILEY-VCH

RESEARCH ARTICLE

Stimuli-responsive supramolecular polymers from amphiphilic phosphodiester-linked azobenzene trimers

Oleh Vybornyi, Shi-Xia Liu and Robert Häner*

Dr. O. Vybornyi, PD Dr. S.-X. Liu and Prof. Dr. R. Häner
Department of Chemistry, Biochemistry and Pharmaceutical Sciences
University of Bern
Freiestrasse 3, CH-3012 Bern, Switzerland
E-mail: robert.haener@unibe.ch

Supporting information for this article is given via a link at the end of the document.

Abstract: An amphiphilic phosphodiester-linked azobenzene trimer has been exploited in the development of stimuli-responsive water-soluble supramolecular polymers. It can reversibly undergo thermal and photoisomerization between *Z* and *E* isomers in EtOH solution. Its self-assembly properties in aqueous medium have been investigated by spectroscopic and microscopic techniques, demonstrating that *E*- and *Z*-azobenzene trimers form supramolecular nanosheets and toroidal nanostructures, respectively. By virtue of the *E*/*Z* photoisomerization of azobenzene units of the trimer, these two different supramolecular morphologies can be switched upon photoirradiation. This finding paves the way towards stimuli-responsive water-soluble supramolecular polymers which hold great promise in the construction of smart functional materials and also in biological applications.

Introduction

The field of supramolecular polymers (SPs) has attracted tremendous interest although it did not emerge as a new branch in polymer science until the late 20th century.[1] SPs are assemblies of repeating building blocks held together by non-covalent interactions.[2] In particular, SPs composed of aromatic amphiphilic building blocks hold great promise in biological applications due to their dynamic nature, unique physical and chemical properties and nanostructures that resemble those of living systems.[3] By virtue of principles of molecular self-assembly, a large diversity of intriguing SPs with unprecedented topologies including 2D nanosheets, 1D nanotubes, vesicles, fibers, toroids and helicoids have been reported.[1e, 4] Among them, stimuli-responsive SPs are of prime importance in the development of smart and adaptive functional materials, ultimately leading to biological functions.[5] Spurred by the exciting results of the light-induced unfolding–refolding of helical coils by mimicking the functions of biopolymers,[4e] we set ourselves the task of preparing an amphiphilic, phosphodiester-linked azobenzene-based trimer for external control over the nanostructures of the resultant SPs. Our keen interest in azobenzene (AZB) derivatives stems from their intriguing structural features and ability to undergo reversible isomerization between *E*- and *Z*- states, triggered by appropriate irradiation, temperature, electric field or mechanical stress.[6] *E*-AZB is planar with a dipole moment of zero while *Z*-AZB is not planar but slightly tilted with a dipole moment of 3.1 D, due to the steric repulsion by the phenyl rings.[7] As a result, the overall length of an AZB core changes from 0.9 nm to 0.55 nm for *E*- and

Z-isomers, respectively, and also the *Z*-isomer is more hydrophilic than the *E*-isomer. Taken together, *E*- and *Z*-isomers are expected to exhibit different self-assembly properties in aqueous environment. As such, AZB has frequently been used to impart responsivity into building blocks that self-assembled into SPs with different properties and diverse nanostructures[8] by changing dimensions and cooperativity of the self-assembly in response to a specific stimulus.[4e, 4f, 9] In close relation with the actual work, electrostatically assembled nanoparticles can, under UV-light irradiation, undergo a significant change in size[10] or shape.[11] As a continuation of our ongoing work, we have prepared an amphiphilic, phosphodiester-linked azobenzene trimer **AZB3** as depicted in Figure 1, which can thermally and photochemically undergo a reversible *E-Z* isomerization. The negative charge of the phosphate group ensures water solubility, while the hydrophobic nature of AZB units facilitates the intramolecular folding and the intermolecular assembly of trimers in an aqueous environment. By a combination of UV-Vis spectroscopy, atomic force microscopy (AFM) and transmission electron microscopy (TEM) techniques, it has been borne out that **E-AZB3** trimers self-assemble into µm-sized 2D nanosheets while **Z-AZB3** trimers form toroidal nanostructures, which undergo a light-triggered reversible interconversion, in stark contrast to the aforementioned nanoassemblies[10-12] in terms of reversibility.
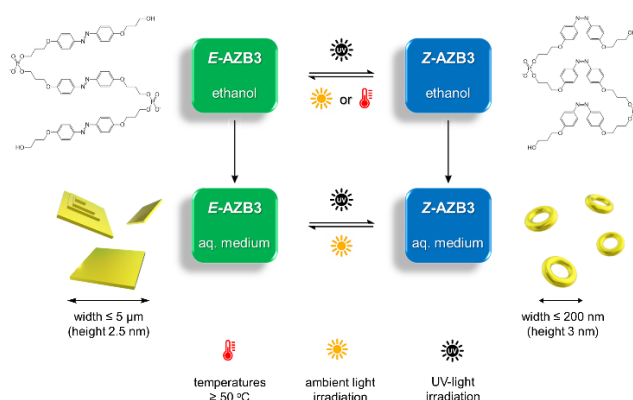

Figure 1. A reversible isomerization of **E-AZB3** to **Z-AZB3** trimer upon UV-light irradiation and *vice versa* upon irradiation with visible light or heating, and light-triggered reversible interconversion of SPs with different morphologies.

Results and Discussion

RESEARCH ARTICLE

The preparation of trimer **AZB3** was accomplished by a solution-phase synthesis[3d, 3e] using an ABZ-functionalized phosphoramidite followed by HPLC purification (supporting information). **AZB3** was kept as a stock solution in ethanol. As it is composed of three azobenzene segments, four isomeric states are expected: *E,E,E*; *E,E,Z*; *E,Z,Z* and *Z,Z,Z*. At room temperature, the stock solution consists of a mixture of these four isomers in a ratio of 47:39:11:3, indicative of a strong predominance of the *E*-isomer (77%). The photoisomerization mechanism can proceed either through out-of-plane rotation of the N=N double bond upon excitation to the bright S_2 ($\pi\pi^*$) state or in-plane inversion at one of the nitrogen atoms upon excitation to the dark S_1 ($n\pi^*$) state.[13] The photoisomerization from the *E*- to *Z*-isomer occurs upon UV-light irradiation at 366 nm[14] and then the back conversion to the *E*-isomer takes place either by heating above 50 °C[15] or, in a slower process, by exposure to ambient light. The isomerization process can be readily monitored by UV-Vis spectroscopy. As depicted in Figure 2, at r.t. predominant *E*-configuration (henceforth **E-AZB3**) which strongly absorbs at 355 nm (black curve), transforms to predominant *Z*-configuration (**Z-AZB3**) upon irradiation at 366 nm (blue curve). The intense absorption bands at 355 nm and 240 nm correspond to the long- and short-axis polarised $\pi \rightarrow \pi^*$ transitions, respectively.[16] A very weak band at 450 nm is attributed to the $n \rightarrow \pi^*$ transition. Clearly, UV-light irradiation of the stock solution for 10 min leads to an increase in the absorbance at 450 nm and a significant decrease in the absorbance at 355 nm, accompanied by a concomitant emergence of a new absorption at 320 nm. These profound spectral changes provide unambiguous evidence for efficient *E-Z* photoisomerization with a photostationary state of 90% *Z*-isomer and 10% *E*-isomer.
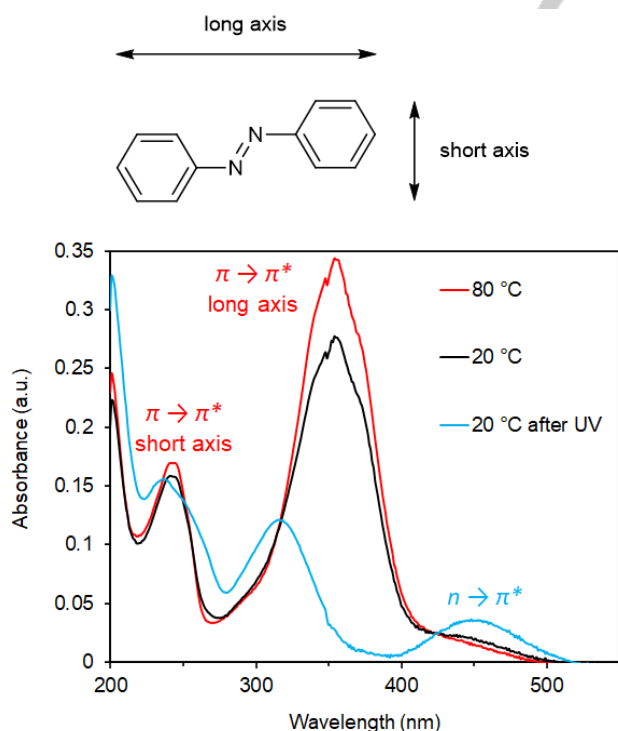
The heating of the solution of **Z-AZB3** (10 min at 80 °C) gives rise to the back conversion to the thermodynamically more stable **E-AZB3** (red curve). The increase in the intensity of the $\pi \rightarrow \pi^*$ band at 80 °C (red) and 20 °C (black) indicates a near quantitative thermal isomerization of *Z*-isomer to *E*-isomer with a photostationary state of 96% *E*-isomer and 4% *Z*-isomer. These results show that the configuration of the trimer **AZB3** in ethanol can be controlled by external forces: at elevated temperatures, it predominantly exists as *E*-isomer, whereas the *Z*-configuration is successfully induced by irradiation at 366 nm.

The self-assembly properties of the described amphiphilic trimer were then studied in a mixture of aqueous buffer (10 mM sodium phosphate buffer at pH 7.2 and 10 mM sodium chloride containing 10% ethanol by volume). As illustrated in Figure 3, the absorption spectrum of **AZB3** at 80 °C (red line) resembles one in ethanol at 20 °C (black line), indicating that **AZB3** exists as a molecularly dissolved trimer, and adopts a random coil structure. Upon cooling down to 20 °C, significant spectral changes (blue line) are observed. Firstly, the long-axis polarised $\pi \rightarrow \pi^*$ band (355 nm) is blue-shifted by 50 nm and experiences a dramatic decrease in intensity, which serves as strong evidence of the formation of *H*-aggregates.[9d, 17] Concomitantly, the short-axis polarised $\pi \rightarrow \pi^*$ band is red-shifted by 10 nm, indicative of the formation of *J*-aggregates.[18] Remarkably, the complete disappearance of the $n \rightarrow \pi^*$ band after cooling the solution in the dark unambiguously manifests the successful conversion of **Z-** to **E-AZB3**.
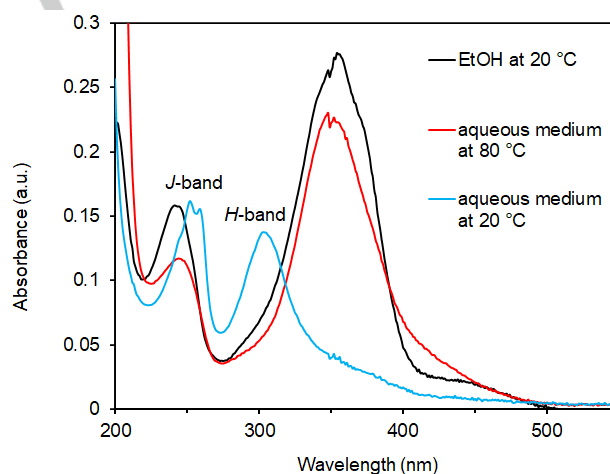
Figure 3. Comparison of UV-Vis absorption spectra of **AZB3** in ethanol at 20 °C (black line), and aqueous medium (10 mM sodium phosphate buffer, pH = 7.2, 10 mM sodium chloride, ethanol 10 vol%) at 80 °C (red line) and 20 °C (blue line); [**AZB3**]: 5 μM.

Figure 2. UV-Vis absorption spectra of **AZB3** recorded in ethanol at ambient conditions (black line), after UV-light irradiation (blue line), and after heating to 80 °C (red line); [**AZB3**]: 5 μM. Top: Illustration of the orientation of electric transition dipole moments (short and long axis).

Figure 4A shows the gradual emergence of an H-band at 305 nm at the expense of the $\pi \rightarrow \pi^*$ absorption band (355 nm) upon slow cooling of the solution from 70 °C to 20 °C, pointing out that supramolecular polymerization occurs *via* a nucleation-elongation process, starting at 65 °C and reaching a plateau at 40 °C.[19] The nanostructures of the formed SPs were investigated by AFM and TEM. As shown by AFM in Figure 4B, the self-assembly leads to the formation of two-dimensionally extended (2D) objects. The nanosheets exhibit a highly regular structure. They extend over several micrometers in length and possess a height of 2.5±0.1 nm (Figure 4C). The shape and micrometer size of SPs is confirmed

2

RESEARCH ARTICLE

by TEM imaging (Figure 4D), showing the sheet-like objects deposited on a carbon-coated holey copper substrate. The formed objects resemble the previously reported nanosheets obtained *via* supramolecular polymerization of amphiphilic pyrene trimers in terms of shape, size, and height.[3c] It can therefore be deduced that in SPs *E-AZB3* trimers are arranged in a stair-like

fashion similar to pyrene trimers, as depicted in Figure 4E. As corroborated by UV-Vis spectra and microscopic imaging, planar *E*-AZB cores stack in a short-slipping *J*-aggregation mode along one direction and in an *H*-aggregation mode along another direction, leading to a 2D polymerization through cooperative nucleation–growth process.
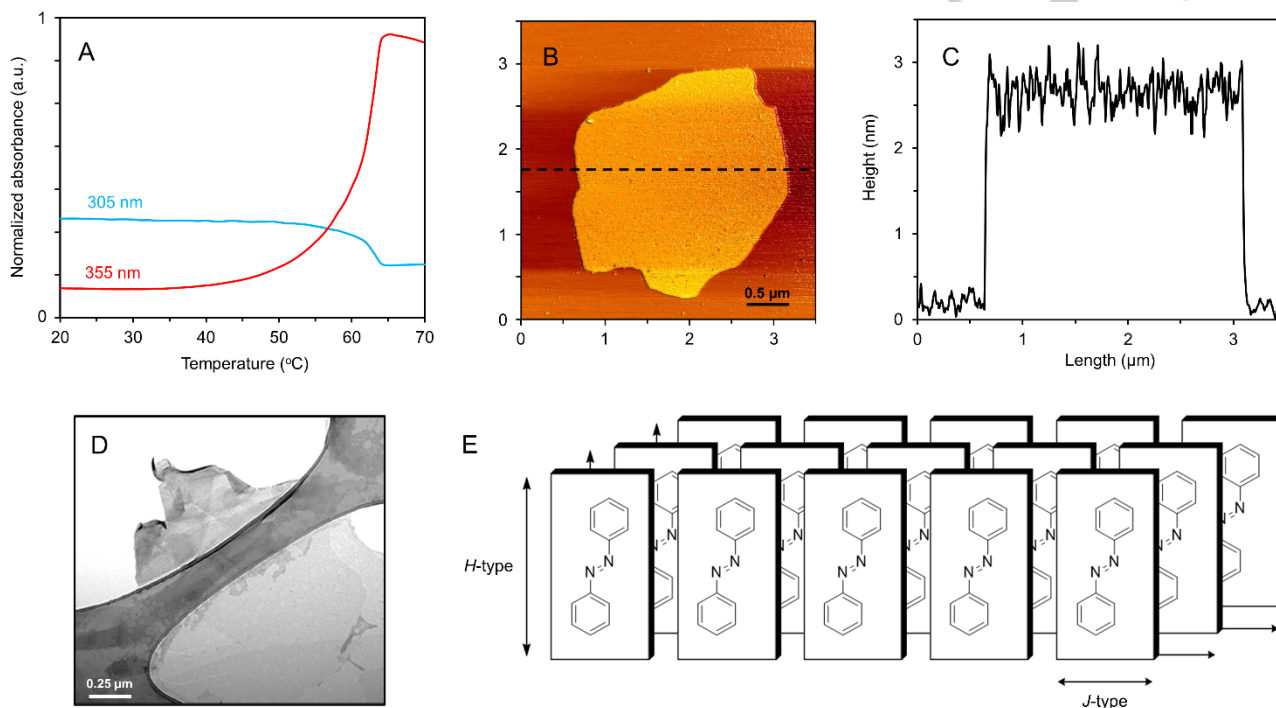

Figure 4. A) Supramolecular polymer formation curve upon cooling of the solution from 70 °C to 20 °C (0.1 °C per minute). B) AFM image of the resultant SPs of *E-AZB3* deposited on APTES-modified mica. C) Height profile of the cross-section line on the AFM image. D) TEM image of SPs of *E-AZB3*. E) Graphical illustration of a stair-like arrangement of *E*-AZB chromophores in supramolecular polymers.

As expected, the cooling gradient has a sizeable impact on the size of the formed SPs.[3a] Fast cooling (10 °C per minute, Figure S1) and slow cooling (0.1 °C per minute, Figures S2 and S3) of the solution from 70 °C to 20 °C results in small (< 1 μm) and large (> 1 μm) nanosheets, respectively. Moreover, the AFM image of the obtained SPs after aging for several days (Figure S1C) shows the imperfection in the nanosheets due to the SPs' dynamic nature.[20]

Next, the spectroscopic and self-assembly properties of *Z-AZB3* are addressed. Two possible ways to obtain self-assembled structures of *Z-AZB3* are demonstrated.

The first strategy involves direct photoisomerization of the previously prepared *E-AZB3* supramolecular polymers upon irradiation under UV-light with 366 nm wavelength. As depicted in Figure 5A, two distinct changes in the absorption spectrum of *E-AZB3* SPs (black line) are observed: a gradual decrease in the intensity of the $\pi \rightarrow \pi^*$ bands with a substantial red-shift of the long-axis polarized band from 305 nm to 320 nm, and the progressive appearance of the $n \rightarrow \pi^*$ transition band over prolonged irradiation time. All these intrinsic spectral signatures indicate the successful photoisomerization from *E-AZB3* to *Z-AZB3*.

It is worth noting, that only solutions with 15% or more ethanol content can undergo *E-Z* photoisomerization. Figure S4 displays

the influence of ethanol content in the medium on the completion of the *E-Z* photoisomerization process. In solutions with less than 15% ethanol, UV-light irradiation leads to negligible changes in the position and intensity of $\pi \rightarrow \pi^*$ bands, suggesting that azobenzene chromophores essentially retain sheet-like molecular assemblies, as evidenced by AFM images (Figure S4). Obviously, 15% ethanol is a prerequisite to the success of this strategy.

The resulting *Z-AZB3* is relatively stable in the absence of visible light or heat sources. As illustrated in Figure 5B, self-assembly of *Z-AZB3* forms toroidal nanostructures with a diameter of approximately 100 nm and a height of 3 nm. In contrast to planar and nonpolar *E*-AZB units, nonplanar and polar *Z*-AZB units show a lower tendency for strong π - π stacks. As such, *Z-AZB3* trimers are likely to form curved stacks leading to the observed toroidal nanostructures, as discussed in the literature for various types of building blocks.[4c, 21] Additional AFM images of the resulting toroids are depicted in Figure S5 (ESI). The presence of nanoobjects in the 50-100 nm range in solution at room temperature was further corroborated by dynamic light scattering (DLS) experiments (ESI, Fig. S6).

An alternative approach to *Z-AZB3* SPs is to add an aliquot of *Z-AZB3*, obtained by photoisomerization after irradiation at 366 nm in ethanol solution, to an aqueous medium followed by gentle mixing. Self-assembly of *Z-AZB3* affords nanostructures (Figures

3

RESEARCH ARTICLE

S7 and S8) with identical diameters and heights to those prepared by the aforementioned *E-Z* photoisomerization process. We, therefore, infer that the addition of an ethanol solution of *Z-AZB3*

produces the spontaneous formation of SPs within minutes at room temperature. Interestingly, the self-assembly occurs without annealing, very probably an isodesmic polymerization occurs.[1a]
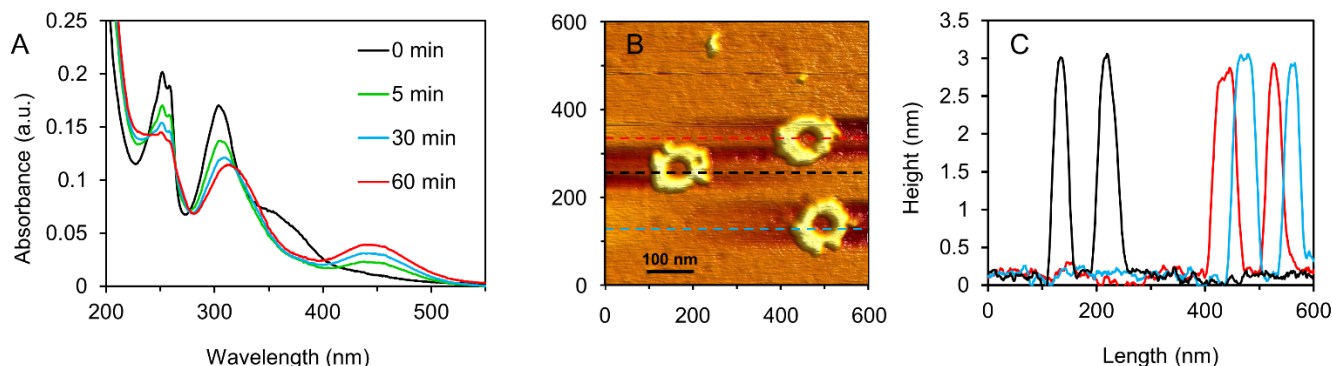

Figure 5. A) Evolution of UV-Vis absorption spectra of *E-AZB3* SPs (black line) in aqueous medium (10 mM sodium phosphate buffer, pH = 7.2, 10 mM sodium chloride, ethanol 15 vol%) monitored after the irradiation with UV-light (366 nm) for 5 min. (green line), 30 min. (blue line) and 60 min. (red line); [*E-AZB3*]: 5 µM. B, C) AFM images alongside the height profile of the *Z-AZB3* nanostructures.

To understand the thermodynamical stability of *Z-AZB3* SPs, temperature-dependent UV-Vis absorption spectra were measured by heating a solution of *Z-AZB3* from 20 °C to 80 °C while keeping it in the dark (Figure 6). Up to 40 °C, the spectrum remains essentially unchanged. Starting from 50 °C on, *Z-* to *E-*isomerization occurs as confirmed by the occurrence of clearly defined isosbestic points at 260 nm, 325 nm and 435 nm. Both absorption bands around 320 nm and 450 nm ($n \rightarrow \pi^*$), characteristics of *Z-AZB3*, decrease at the benefit of a strong $\pi \rightarrow \pi^*$ absorption band at 355 nm, characteristics of *E-AZB3*. Thus, under the exclusion of light below 40 °C *Z-AZB3* SPs are preserved, which then undergo disassembly and thermal isomerization to the molecularly dissolved *E-AZB3* with further increase of the temperature.
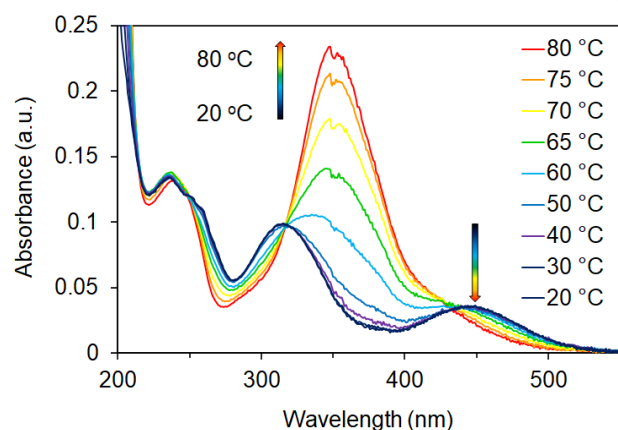
function of exposure time with appropriate light irradiation. UV-Vis absorption measurements have been performed with great caution to avoid undesired thermal conversion after different exposure times (Figure 7). Upon exposure of freshly prepared *Z-AZB3* (red line) to ambient light for 30 min, significant changes are observed (blue line). A profound decrease in the $n \rightarrow \pi^*$ absorption band accompanied with the appearance of *J*-band (250 nm) and *H*-band (305 nm) demonstrates the direct conversion of *Z-AZB3* SPs into *E-AZB3* SPs. Upon photo-irradiation for 120 min, no further noticeable spectral changes are observed. The final spectrum resembles that of *E-AZB3* SPs (blue line in Figure 3). Irradiation of *Z-AZB3* SPs at 427 nm using an LED lamp further shows that *Z*-to-*E* isomerization promotes the disassembly of the toroidal nanostructures and the temporary appearance of ill-defined aggregates. Further progression finally leads to the reassembly of the dissolved *E-AZB3* into the nanosheets (see SI, Figure S9).

Interestingly, multi-layered nanosheets are formed after exposure of *Z-AZB3* solution to ambient light at room temperature for 15 min, as shown in Figure 8 and Figure S10. At this point, the two individual SP morphologies (toroids on the surface of the nanosheets) are co-existing, indicating the ongoing *Z*-to-*E* photoisomerization process. The height profile of the resulting nanostructures confirms that layers with a uniform thickness of ca. 2.5 nm are arranged on top of each other. The size of each layer is smaller than the one below, indicating that individual nanosheets are formed on top of an already existing one.–As demonstrated above, the hydrophobic intermolecular interactions in the forms of *J*- and *H*-aggregation act cooperatively in two dimensions, leading to the formation of nanosheets upon self-assembly of *E-AZB3*. In contrast, non-planar and polar *Z*-AZB units cannot stack in an *H*-aggregation fashion due to their steric hindrance and dipole-dipole interactions forming curved stacks *via J*-aggregations. Isomerization to *E*-AZB enables nucleated *H*-aggregation, which changes the internal order and reduces the spontaneous curvature. We hypothesize that the primary nucleation process takes place simultaneously with the growth process. During the photoisomerization process, *Z-AZB3* toroids

Figure 6. Temperature-dependent UV-Vis absorption spectra of *Z-AZB3* in an aqueous medium (10 mM sodium phosphate buffer, pH = 7.2, 10 mM sodium chloride, ethanol 15 vol%) measured after the equilibration for 5 min at each temperature (solutions kept in the dark); [*Z-AZB3*]: 5 µM.

The photostability and reversibility properties of SPs have been investigated by monitoring the absorption spectral changes as a

4

that are adsorbed on already existing nanosheets undergo transformation into small *E-AZB3* nanosheets that serve as templates for the subsequent transformation of additional *Z-AZB3* toroids.
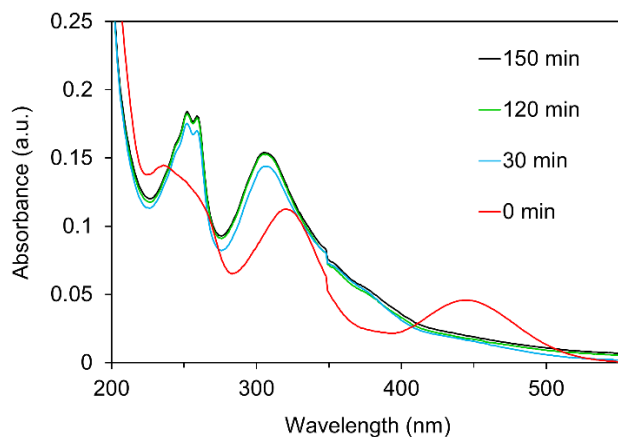

Figure 7. Evolution of UV-Vis absorption spectra of *Z-AZB3* (red line) in an aqueous medium (10 mM sodium phosphate buffer, pH = 7.2, 10 mM sodium chloride, ethanol 15 vol%) monitored after exposure to ambient light for 30 min. (blue line), 120 min. (green line) and 150 min. (black line); [*Z-AZB3*]: 5 μM.
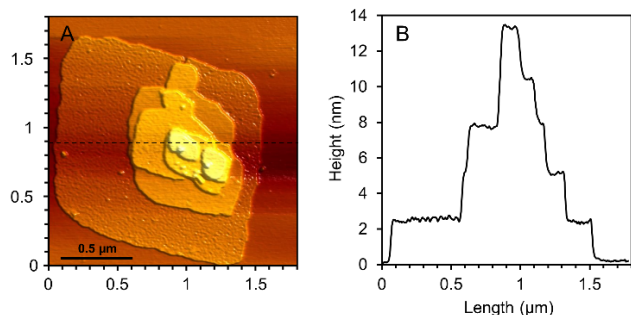

Figure 8. A) AFM image of multi-layered nanosheets formed after the photoisomerization from *Z-AZB3* to *E-AZB3* at ambient light conditions. B) Height profile of the cross-section on the AFM image.

Conclusion

In conclusion, the present paper summarizes the preparation and self-assembly properties of a novel stimuli-responsive amphiphilic AZB-based trimer. Thermal and photoisomerization of AZB units within the resultant SPs and molecularly dissolved trimers *AZB3* has been investigated. The initial mixture of configurational isomers of *AZB3* in ethanol is converted into *E-AZB3* at temperatures above 50 °C or, alternatively, into *Z-AZB3* by irradiation with UV-light at temperatures below 50 °C. In aqueous medium, *E-AZB3* trimers self-assemble into μm-sized 2D nanosheets while *Z-AZB3* trimers form toroidal nanostructures. Both nanosheets and toroids can be thermally disassembled (≥ 50 °C). Photoisomerization of the AZB units by exposure to UV or visible light provides a means to reversibly destroy or recover 2D nanosheets. The obtained μm-sized 2D nanosheets of *E-AZB3* can undergo UV-light-induced photoisomerization in an aqueous

medium to form *Z-AZB3* toroidal structures. During the photoisomerization from *Z-AZB3* to *E-AZB3*, multi-layered nanosheets with a uniform height are observed. This report paves the way towards new, stimuli-responsive water-soluble SPs which are of prime importance in the development of smart functional materials.

[1] a) M. F. J. Mabesoone, A. R. A. Palmans, E. W. Meijer, *J. Am. Chem. Soc.* **2020**, *142*, 19781-19798; b) T. Aida, E. W. Meijer, *Isr. J. Chem.* **2020**, *60*, 33-47; c) L. Brunsveld, B. J. B. Folmer, E. W. Meijer, R. P. Sijbesma, *Chem. Rev.* **2001**, *101*, 4071-4098; d) T. F. A. De Greef, M. M. J. Smulders, M. Wolffs, A. P. H. J. Schenning, R. P. Sijbesma, E. W. Meijer, *Chem. Rev.* **2009**, *109*, 5687-5754; e) L. Yang, X. Tan, Z. Wang, X. Zhang, *Chem. Rev.* **2015**, *115*, 7196-7239; f) M. Vybornyi, Y. Vyborna, R. Häner, *Chem. Soc. Rev.* **2019**, *48*, 4347-4360.

[2] a) F. Zapata, L. González, A. Bastida, D. Bautista, A. Caballero, *Chem. Commun.* **2020**, *56*, 7084-7087; b) M. Hartlieb, E. D. H. Mansfield, S. Perrier, *Polym. Chem.* **2020**, *11*, 1083-1110; c) O. Goor, S. I. S. Hendrikse, P. Y. W. Dankers, E. W. Meijer, *Chem. Soc. Rev.* **2017**, *46*, 6621-6637; d) X. Ma, H. Tian, *Acc. Chem. Res.* **2014**, *47*, 1971-1981; e) J. D. Tovar, *Acc. Chem. Res.* **2013**, *46*, 1527-1537.

[3] a) M. Vybornyi, A. Rudnev, R. Häner, *Chem. Mater.* **2015**, *27*, 1426-1431; b) M. Vybornyi, H. Yu, R. Häner, *Chimia* **2019**, *73*, 468-472; c) M. Vybornyi, A. V. Rudnev, S. M. Langenegger, T. Wandlowski, G. Calzaferri, R. Häner, *Angew. Chem. Int. Ed.* **2013**, *52*, 11488-11493; d) P. W. Münich, M. Pfäffli, M. Volland, S.-X. Liu, R. Häner, D. M. Guldi, *Nanoscale* **2020**, *12*, 956-966; e) S. Rothenbühler, C. D. Bösch, S. M. Langenegger, S.-X. Liu, R. Häner, *Org. Biomol. Chem.* **2018**, *16*, 6886-6889; f) A. V. Rudnev, V. L. Malinovskii, A. L. Nussbaumer, A. Mishchenko, R. Häner, T. Wandlowski, *Macromolecules* **2012**, *45*, 5986-5992; g) A. L. Nussbaumer, D. Studer, V. L. Malinovskii, R. Häner, *Angew. Chem. Int. Ed.* **2011**, *50*, 5490-5494; h) D. D. Prabhu, K. Aratsu, Y. Kitamoto, H. Ouchi, T. Ohba, M. J. Hollamby, N. Shimizu, H. Takagi, R. Haruki, S.-i. Adachi, S. Yagai, *Sci. Adv.* **2018**, *4*, eaat8466; i) T. Kim, J. Y. Park, J. Hwang, G. Seo, Y. Kim, *Adv. Mater.* **2020**, *32*, 2002405.

[4] a) N. Sasaki, M. F. J. Mabesoone, J. Kikkawa, T. Fukui, N. Shioya, T. Shimoaka, T. Hasegawa, H. Takagi, R. Haruki, N. Shimizu, S.-i. Adachi, E. W. Meijer, M. Takeuchi, K. Sugiyasu, *Nat. Commun.* **2020**, *11*, 3578; b) S. Datta, Y. Kato, S. Higashiharaguchi, K. Aratsu, A. Isobe, T. Saito, D. D. Prabhu, Y. Kitamoto, M. J. Hollamby, A. J. Smith, R. Dalgliesh, N. Mahmoudi, L. Pesce, C. Perego, G. M. Pavan, S. Yagai, *Nature* **2020**, *583*, 400-405; c) S. Yagai, Y. Goto, X. Lin, T. Karatsu, A. Kitamura, D. Kuzuhara, H. Yamada, Y. Kikkawa, A. Saeki, S. Seki, *Angew. Chem. Int. Ed.* **2012**, *51*, 6643-6647; d) M. J. Hollamby, K. Aratsu, B. R. Pauw, S. E. Rogers, A. J. Smith, M. Yamauchi, X. Lin, S. Yagai, *Angew. Chem. Int. Ed.* **2016**, *55*, 9890-9893; e) B. Adhikari, Y. Yamada, M. Yamauchi, K. Wakita, X. Lin, K. Aratsu, T. Ohba, T. Karatsu, M. J. Hollamby, N. Shimizu, H. Takagi, R. Haruki, S.-i. Adachi, S. Yagai, *Nat. Commun.* **2017**, *8*, 15254; f) B. Adhikari, K. Aratsu, J. Davis, S. Yagai, *Angew. Chem. Int. Ed.* **2019**, *58*, 3764-3768; g) E. Krieg, M. M. C. Bastings, P. Besenius, B. Rybtchinski, *Chem. Rev.* **2016**, *116*, 2414-2477; h) G. Gröger, W. Meyer-Zaika, C. Böttcher, F. Gröhn, C. Ruthard, C. Schmuck, *J. Am. Chem. Soc.* **2011**, *133*, 8961-8971.

[5] a) X. Yan, F. Wang, B. Zheng, F. Huang, *Chem. Soc. Rev.* **2012**, *41*, 6042-6065; b) M. Baroncini, J. Groppi, S. Corra, S. Silvi, A. Credi, *Adv.*

Opt. Mater. **2019**, *7*, 1900392; c) L. C. Palmer, S. I. Stupp, *Acc. Chem. Res.* **2008**, *41*, 1674-1684.

[6]   a) H. M. D. Bandara, S. C. Burdette, *Chem. Soc. Rev.* **2012**, *41*, 1809-1825; b) G. S. Hartley, *Nature* **1937**, *140*, 281-281; c) A. S. Oshchepkov, S. S. R. Namashivaya, V. N. Khrustalev, F. Hampel, D. N. Laikov, E. A. Kataev, *J. Org. Chem.* **2020**, *85*, 9255-9263; d) A. A. Beharry, G. A. Woolley, *Chem. Soc. Rev.* **2011**, *40*, 4422-4437.

[7]   a) A. Mostad, C. R⁻mming, S. Hammarstr^m, R. J. Lousberg, U. Weiss, *Acta Chem. Scand.* **1971**, *25*, 3561-3568; b) C. Brown, *Acta Crystallogr.* **1966**, *21*, 146-152.

[8]   a) K. Tamaki, S. Datta, K. Tashiro, A. Isobe, F. Silly, S. Yagai, *Asian J. Org. Chem.* **2021**, *10*, 257-261; b) S. Geng, Y. Wang, L. Wang, T. Kouyama, T. Gotoh, S. Wada, J.-Y. Wang, *Sci. Rep.* **2017**, *7*, 39202; c) T. Saito, S. Yagai, *Eur. J. Org. Chem.* **2020**, *2020*, 2475-2478; d) T. Saito, S. Yagai, *Org. Biomol. Chem.* **2020**, *18*, 3996-3999.

[9]   a) E. Fuentes, M. Gerth, J. A. Berrocal, C. Matera, P. Gorostiza, I. K. Voets, S. Pujals, L. Albertazzi, *J. Am. Chem. Soc.* **2020**, *142*, 10069-10078; b) T. Hirose, F. Helmich, E. W. Meijer, *Angew. Chem. Int. Ed.* **2013**, *52*, 304-309; c) P. Duan, Y. Li, L. Li, J. Deng, M. Liu, *J. Pyhs. Chem. B* **2011**, *115*, 3322-3329; d) S. Ma, S. Kurihara, Y. Tomimori, S. Kim, E. Kwon, A. Muramatsu, K. Kanie, *RSC Adv.* **2020**, *10*, 32984-32991; e) N. A. Simeth, S. Kobayashi, P. Kobauri, S. Crespi, W. Szymanski, K. Nakatani, C. Dohno, B. L. Feringa, *Chem. Sci.* **2021**, *12*, 9207-9220.

[10]   I. Willerich, F. Gröhn, *Angew. Chem. Int. Ed.* **2010**, *49*, 8104-8108.

[11]   G. Mariani, A. Krieger, D. Moldenhauer, R. Schweins, F. Gröhn, *Macromol. Rapid. Comm.* **2018**, *39*, 1700860.

[12]   I. Willerich, F. Gröhn, *Macromolecules* **2011**, *44*, 4452-4461.

[13]   a) C. J. Otolski, A. M. Raj, V. Ramamurthy, C. G. Elles, *Chem. Sci.* **2020**, *11*, 9513-9523; b) C. R. Crecca, A. E. Roitberg, *J. Phys. Chem. A* **2006**, *110*, 8188-8203.

[14]   a) S. Crespi, N. A. Simeth, B. Koenig, *Nat. Rev. Chem.* **2019**, *3*, 133-146; b) Ľ. Vetráková, V. Ladányi, J. Al Anshori, P. Dvořák, J. Wirz, D. Heger, *Photochem. Photobiol. Sci.* **2017**, *16*, 1749-1756.

[15]   a) T. Asano, T. Okada, S. Shinkai, Y. Kusano, O. Manabe, *J. Am. Chem. Soc.* **1981**, *103*, 5161-5165; b) P. Bortolus, S. Monti, *J. Phys. Chem.* **1979**, *83*, 648-652.

[16]   a) C. L. Forber, E. C. Kelusky, N. J. Bunce, M. C. Zerner, *J. Am. Chem. Soc.* **1985**, *107*, 5884-5890; b) M. Shimomura, R. Ando, T. Kunitake, *Ber. Bunsen-Ges. Phys. Chem.* **1983**, *87*, 1134-1143; c) D. L. Beveridge, H. H. Jaffé, *J. Am. Chem. Soc.* **1966**, *88*, 1948-1953; d) R. M. Hochstrasser, S. K. Lower, *J. Chem. Phys.* **1962**, *36*, 3505-3506.

[17]   a) X. Song, J. Perlstein, D. G. Whitten, *J. Am. Chem. Soc.* **1997**, *119*, 9144-9159; b) T. Kawasaki, M. Tokuhiro, N. Kimizuka, T. Kunitake, *J. Am. Chem. Soc.* **2001**, *123*, 6792-6800.

[18]   a) M. Shimomura, S. Aiba, N. Tajima, N. Inoue, K. Okuyama, *Langmuir* **1995**, *11*, 969-976; b) I. Zebger, M. Rutloh, U. Hoffmann, J. Stumpe, H. W. Siesler, S. Hvilsted, *J. Phys. Chem. A* **2002**, *106*, 3454-3462.

[19]   a) P. Jonkheijm, P. van der Schoot, A. P. H. J. Schenning, E. W. Meijer, *Science* **2006**, *313*, 80; b) P. A. Korevaar, S. J. George, A. J. Markvoort, M. M. J. Smulders, P. A. J. Hilbers, A. P. H. J. Schenning, T. F. A. De Greef, E. W. Meijer, *Nature* **2012**, *481*, 492-496.

[20]   T. F. A. de Greef, E. W. Meijer, *Nature* **2008**, *453*, 171-173.

[21]   a) H. Shao, J. Seifert, N. C. Romano, M. Gao, J. J. Helmus, C. P. Jaroniec, D. A. Modarelli, J. R. Parquette, *Angew. Chem. Int. Ed.* **2010**, *49*, 7688-7691; b) H. Wang, M. Lee, *Macromol. Rapid. Comm.* **2020**, *41*, 2000138; c) S. Yagai, M. Yamauchi, A. Kobayashi, T. Karatsu, A. Kitamura, T. Ohba, Y. Kikkawa, *J. Am. Chem. Soc.* **2012**, *134*, 18205-18208.

6

RESEARCH ARTICLE

Entry for the Table of Contents

Insert graphic for Table of Contents here.
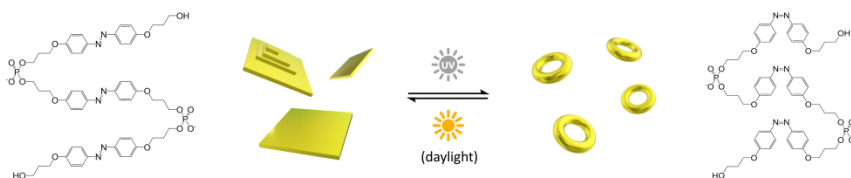
The assembly of stimuli-responsive supramolecular polymers (SPs) of amphiphilic oligomers in aqueous medium is presented. Azobenzene-derived oligophosphates undergo morphological transformation upon light-triggered isomerization. In a reversible process, sheet-like SPs are switched to toroid-shaped objects by changing the configuration of the building blocks.

Institute and/or researcher Twitter usernames: @DCBPunibern